

Tungsten oxide/tungsten nanocrystals for nonvolatile memory devices

C. H. Chen, T. C. Chang, I. H. Liao, P. B. Xi, Joe Hsieh, Jason Chen, Tensor Huang, S. M. Sze, U. S. Chen, and J. R. Chen

Citation: [Applied Physics Letters](#) **92**, 013114 (2008); doi: 10.1063/1.2822401

View online: <http://dx.doi.org/10.1063/1.2822401>

View Table of Contents: <http://scitation.aip.org/content/aip/journal/apl/92/1?ver=pdfcov>

Published by the [AIP Publishing](#)

Articles you may be interested in

[NiSiGe nanocrystals for nonvolatile memory devices](#)

Appl. Phys. Lett. **94**, 062102 (2009); 10.1063/1.3080201

[Nonvolatile memory devices with high density ruthenium nanocrystals](#)

Appl. Phys. Lett. **93**, 242102 (2008); 10.1063/1.3049598

[Tungsten nanocrystal memory devices improved by supercritical fluid treatment](#)

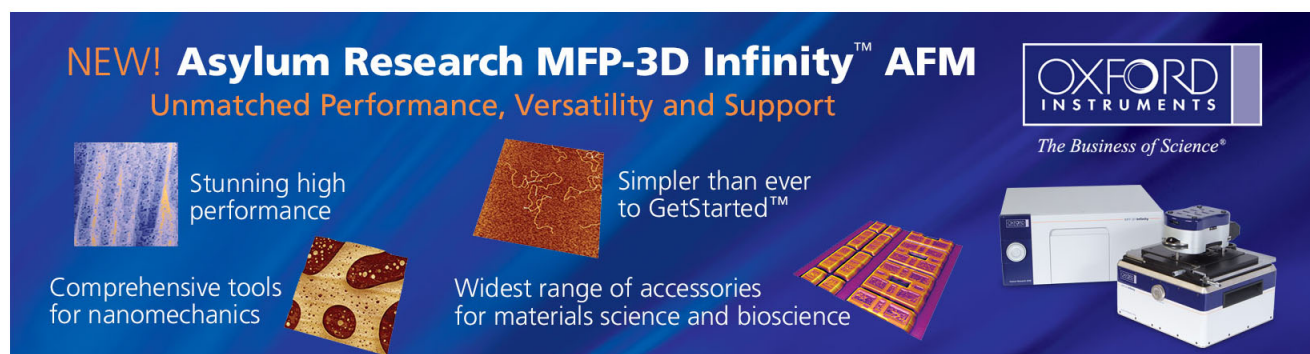
Appl. Phys. Lett. **91**, 232104 (2007); 10.1063/1.2803937

[Minimization of germanium penetration, nanocrystal formation, charge storage, and retention in a trilayer memory structure with silicon nitride/hafnium dioxide stack as the tunnel dielectric](#)

Appl. Phys. Lett. **84**, 4385 (2004); 10.1063/1.1757022

[Effect of germanium concentration and tunnel oxide thickness on nanocrystal formation and charge storage/retention characteristics of a trilayer memory structure](#)

Appl. Phys. Lett. **83**, 3558 (2003); 10.1063/1.1615840

The advertisement features a dark blue background with white and orange text. At the top left, it reads 'NEW! Asylum Research MFP-3D Infinity™ AFM' in large white letters, followed by 'Unmatched Performance, Versatility and Support' in orange. To the right is the Oxford Instruments logo, which includes the text 'OXFORD INSTRUMENTS' and the tagline 'The Business of Science®'. Below the main text are four images: a textured surface, a circular pattern, a grid of small squares, and the physical AFM instrument. Each image is accompanied by a short text description: 'Stunning high performance', 'Simpler than ever to GetStarted™', 'Comprehensive tools for nanomechanics', and 'Widest range of accessories for materials science and bioscience'.

Tungsten oxide/tungsten nanocrystals for nonvolatile memory devices

C. H. Chen

Department of Materials Science and Engineering, National Tsing Hua University, Hsinchu, Taiwan 300, Republic of China

T. C. Chang^{a)}

Department of Physics and Institute of Electro-Optical Engineering, and Center for Nanoscience and Nanotechnology, National Sun Yat-Sen University, Kaohsiung, 804 Taiwan, Republic of China

I. H. Liao

ProMOS Technologies, No. 19, Li Hsin Rd., Science-Based Industrial Park, Hsinchu, Taiwan 300, Republic of China

P. B. Xi

Institute of Electro-Optical Engineering, National Sun Yat-Sen University, Kaohsiung, Taiwan 804, Republic of China

Joe Hsieh, Jason Chen, and Tensor Huang

ProMOS Technologies, No. 19, Li Hsin Rd., Science-Based Industrial Park, Hsinchu, Taiwan 300, Republic of China

S. M. Sze

Institute of Electronics, National Chiao Tung University, Taiwan, Hsinchu, Taiwan 300, Republic of China

U. S. Chen and J. R. Chen

Department of Materials Science and Engineering, National Tsing Hua University, Hsinchu, Taiwan 300, Republic of China

(Received 13 July 2007; accepted 16 November 2007; published online 7 January 2008)

In this work, the fabrication of WO_3/W nanocrystals for nonvolatile memory devices has been achieved via rapid thermal oxidation of tungsten silicide. Amorphous Si and WSi_x ($x=2.7$) layers were deposited onto the tunneling oxide and sequentially oxidized to form well-shaped WO_3/W nanocrystals. The mean size of WO_3/W nanocrystals is ~ 8.4 nm, while density is $\sim 1.57 \times 10^{11} \text{ cm}^{-2}$. Moreover, the nonvolatile memory device for WO_3/W nanocrystals exhibits ~ 0.53 V threshold voltage shift under 1 V/(-5 V) operation. The sample without capping *a*-Si layer was also fabricated for comparison. By material analyses, reasonable formation mechanisms are proposed in this letter. © 2008 American Institute of Physics. [DOI: 10.1063/1.2822401]

In recent years, extensive articles have been published relating with nanocrystal application on nonvolatile memory devices. The memory devices employing distributed nanocrystals as storage elements have exhibited outstanding performance in high speed and low power consumption so that it has been regarded as a candidate to replace conventional dynamic random array memories and/or flash memories.¹⁻³ Theoretically, metal nanocrystals possess more advantages than other materials for nonvolatile memory devices, such as a wide range of available work functions, higher density of states, and smaller energy perturbation due to carrier confinement.⁴⁻⁶ However, few metal materials could be employed in manufacture of current semiconductor industry because of incompatibilities with various processes. Among the practicable metals for semiconductor industry, tungsten provides excellent physical as well as electrical properties for satisfaction of both requirements. For example, high melting point prevents deformation at high temperature, high work function provides high density of states for electrons trapping, chemical stability with Si atom, and so on.^{7,8}

In this letter, the fabrication of well-shaped WO_3/W nanocrystals embedded in SiO_2 for nonvolatile memory device application has been demonstrated. Additionally, the failure mechanism of imperfect WO_3/W nanocrystal-based

nonvolatile memory without capping *a*-Si layer is discussed as well.

8 in. (100) oriented *p*-type silicon wafers were chemically cleaned by a standard RCA procedure, followed a 3 nm tunnel oxide was grown in a rapid thermal anneal system. Subsequently, a 4-nm-thick WSi_x ($x=2.7$) layer was deposited onto the tunnel oxide using chemical vapor deposition system. An amorphous Si layer (*a*-Si, 5 nm) was capped onto the tungsten silicide layer to provide sufficient Si atoms for forming the control oxide layer. Afterward, a dry oxidation was utilized for the formation of the control oxide at 900–1100 °C and WO_3/W nanocrystals were precipitated in the matrix of SiO_2 as well. In addition, the sample without capping *a*-Si layer was also oxidized in the same conditions. Chemical compositions of samples were investigated by x-ray photoelectron spectrometry (XPS) (Physical Electronics PHI 1600) with Mg $K\alpha$ (energy=1253.6 eV) radiation. Finally, Al gate electrode was patterned and sintered. The structural analyses were performed by transmission electron microscopy (TEM). The capacitance-voltage (*C-V*) measurements were performed by a precision LCR meter (HP4284A) to observe the memory characteristics of WO_3/W nanocrystal-based devices.

Figure 1(a) shows the cross-sectional TEM image of $\text{WSi}_x/\text{SiO}_2/\text{Si}$ structure for RTO process. An about 150 nm cluster was observed on the tunneling oxide. The clusters

^{a)}Electronic mail: techang@mail.phys.nsysu.edu.tw.

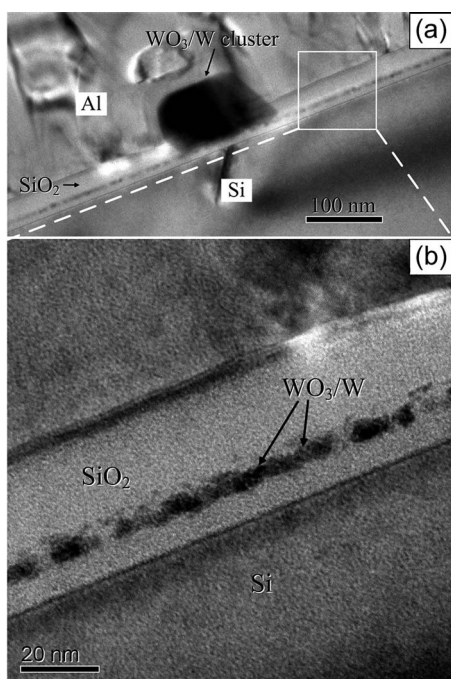


FIG. 1. (a) Cross-section TEM micrograph of $WSi_x/SiO_2/Si$ structure for rapid thermal oxidation treatment and (b) locally magnifying image from Fig. 1(a)

appear repeatedly on the sample every several micrometers. Besides, the dark contrast in TEM suggests that it was composed of tungsten and/or tungsten compounds. The square shows a highlighted high-resolution TEM (HRTEM) image from the Fig. 1(a). WO_3/W nanocrystals are conspicuously observed embedded in SiO_2 matrix, while the nanocrystals are segregated imperfectly in shape.

In order to improve the formation of imperfect-shaped nanocrystals aforementioned, a 5 nm a -Si layer was capped on WSi_x layer and followed oxidizing in the same conditions. The inset of Fig. 2(a) represents the HRTEM image of oxidized a -Si/ $WSi_x/SiO_2/Si$ structure. It displays that the WO_3/W nanocrystals were formed into distributed- and well-shaped ellipsoids. The confirmation of mean size of WO_3/W nanocrystals is approximately 8.4 nm in diameter. Figure 2(a) shows the density of WO_3/W nanocrystals versus rapid thermal oxidation (RTO) time. At initially 30 s, WO_3/W nanocrystals nucleated rapidly and sequentially coarsened. As RTO performed at 60 s, the density of WO_3/W nanocrystals decreases to $1.57 \times 10^{11} \text{ cm}^{-2}$, and there is no obvious variation from 60 to 120 s. The C - V characteristics of WO_3/W nanocrystals embedded in oxide are shown in Fig. 2(b). While the voltage swept from 1 to -5 V and back to 1 V, a threshold-voltage shift of 0.53 V was observed, which is sufficient to be defined as “1” or “0” for the logic-circuit design.

XPS was used to determine the chemical nature of the a -Si/ $WSi_x/SiO_2/Si$ sample which was oxidized for 120 s RTO process. Ar sputtering for 100 sec is utilized for cleaning. Figure 3 presents the XPS spectra of W 4f. The peaks centered at 3.14 and 33.4 eV were identified as W 4f_{7/2} and W 4f_{5/2}, respectively. Slight WO_3 chemical states were observed at 35.8 and 37.8 eV as well.⁹ Nevertheless, Si atoms in the sample are mostly oxidized, which the evidence is SiO_2 signal identified from Si 2p XPS spectra. Because of extremely little solid solubility of O atoms within W

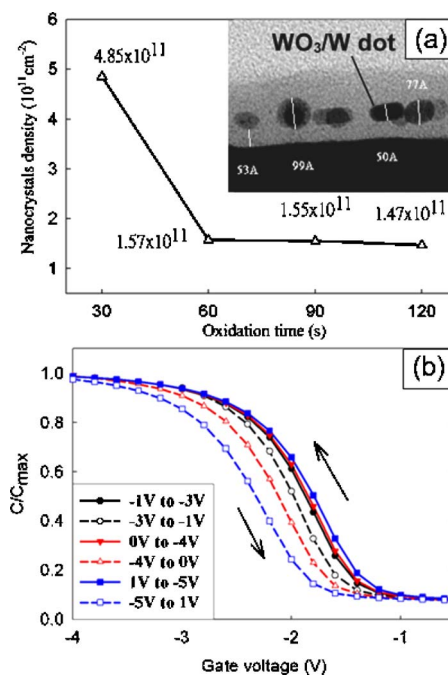


FIG. 2. (Color online) (a) The variation of WO_3/W nanocrystals density vs RTO process time. The inset is the cross-section TEM micrograph of a -Si/ $WSi_x/SiO_2/Si$ structure for RTO treatment. (b) The capacitance-voltage (C - V) hysteresis of WO_3/W nanocrystals memory device after bi-directional sweeps between $(-1 \text{ V})/(-3 \text{ V})$, $0 \text{ V}/(-4 \text{ V})$, and $1 \text{ V}/(-5 \text{ V})$.

material,¹⁰ O atoms could not exist in W nanocrystals except absolutely oxidation of tungsten. Therefore, it is a reasonable speculation that the position of WO_3 should be on the surface of W nanocrystals. Namely, W nanocrystals are encapsulated by a very thin WO_3 layer.

To elucidate the appearance of samples with and without a -Si layer, a schematic diagram is shown in Fig. 4. Initially, tungsten silicide is oxidized and decomposes to W and Si.^{11,12} Both elements transform to oxygen compounds simultaneously. Comparing with the oxides of W and Si, the heats of formation per oxygen atom are -67.1 kcal/mole for WO_3 and -73.0 kcal/mole for SiO_2 , respectively.⁷ It is reasonable to believe that the primitive oxidation mostly arises with Si atoms, and only slight W atoms are transformed into W oxides.¹³ At the same time, tungsten also aggregates to diminish free energy of surface. However, WO_3 is not stable at high temperature. Some WO_3 vaporized during the nucle-

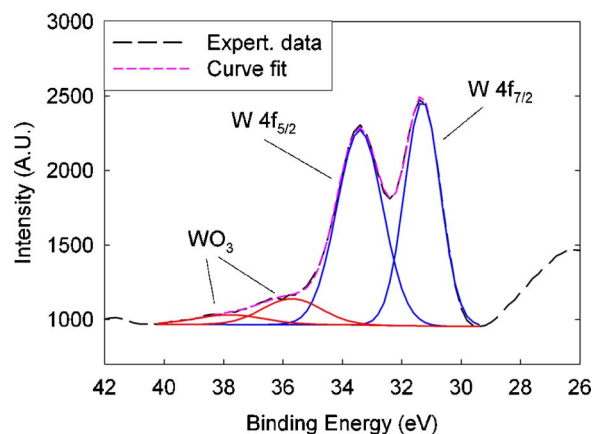


FIG. 3. (Color online) The W 4f XPS spectra of a -Si/ $WSi_x/SiO_2/Si$ sample for RTO process. The sample was performed after 100 s Ar sputtering.

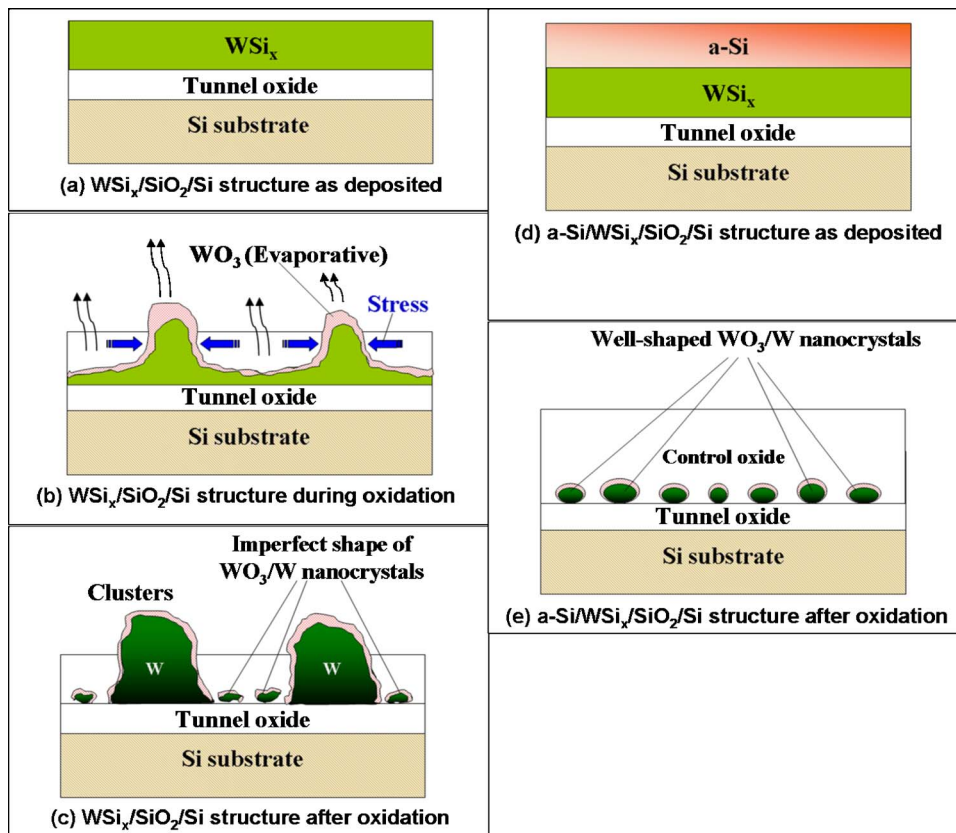


FIG. 4. (Color online) Schematic diagram of the rapid thermal oxidation process. (a) $WSi_x/SiO_2/Si$ structure as deposited. (b) During oxidation. (c) Imperfect nanocrystals formed after oxidation. (d) $a-Si/WSi_x/SiO_2/Si$ structure as deposited. (e) Well-shaped WO_3/W nanocrystals embedded in SiO_2 after oxidation.

ation, thus the imperfect shape of WO_3/W nanocrystals formed, as shown from Fig. 4(a) to Fig. 4(c). It is confirmed in Fig. 1(b). Furthermore, difference thermal expansion coefficients are induced between the tunneling oxide and W silicide (0.5 ppm/°C for SiO_2 and 12.5 ppm/°C for WSi_2). W silicide film is compressed by thermal stress during thermal oxidation process. The stress attributes to enhance the aggregation of the WO_3/W and results in clustered, as shown in Fig. 1(a).

Because the cluster formation is due to raising a violent thermal stress in a W silicide film during oxidation, WO_3/W nanocrystals must be precipitated before the W silicide film reacts with oxygen to alleviate the cluster formation. Capping an $a-Si$ layer on W silicide film, as shown in Fig. 4(d), is a significant way to retard oxygen diffusing into the W silicide film. First, an upper $a-Si$ layer is beneficial to reduce the formation of stress at high temperature. Moreover, great parts of SiO_2 are transformed from $a-Si$ capping layer during oxidation. Oxide layer also moderates the diffusion of oxygen into W silicide. The delay time of the W oxidation makes the decomposed W atoms to aggregate completely, as shown in Fig. 4(e). Even if tungsten is slightly oxidized, the thin SiO_2 layer also plays a significant role in keeping WO_3 from evaporation. Capping $a-Si$ layer onto W silicide before oxidation indeed results in perfect shape of WO_3/W nanocrystals.

In summary, the fabrication of WO_3/W nanocrystals as memory devices by oxidizing $a-Si/WSi_x/SiO_2/Si$ structure has been achieved. The nonvolatile memory device with WO_3/W nanocrystals exhibits ~ 0.53 V threshold voltage shift under 1 V/(-5 V) operation. Meanwhile, the mechanisms of formation of WO_3/W nanocrystals also are pro-

posed. Volatile WO_3 and excessive stress lead to the production of imperfect nanocrystals without capping an $a-Si$ layer. The implementation of the present structure is compatible as well as practicable for nonvolatile memory technology.

This work was performed at National Nano Device Laboratory and was supported by the National Science Council of the Republic of China under Contract Nos. NSC 96-2120-M-110-001 and NSC 95-2221-E-009-296-MY2. Also, the authors thank the ProMOS Technologies, Taiwan, for their support.

¹S. Tiwari, F. Rana, K. Chan, H. Hanafi, C. Wei, and D. Buchanan, Tech. Dig. - Int. Electron Devices Meet. **1995**, 521.

²Z. Liu, C. Lee, V. Narayanan, G. Pei, and E. C. Kan, IEEE Trans. Electron Devices **49**, 1606 (2002).

³A. Thean and J. P. Leburton, IEEE Potentials **21**, 35 (2002).

⁴P. H. Yeh, L. J. Chen, P. T. Liu, D. Y. Wang, and T. C. Chang, Electrochim. Acta **52**, 2920 (2007).

⁵S. S. Kwang, S. J. Choi, J. Y. Choi, E. J. Jang, B. K. Kim, S. J. Park, D. G. Cha, I. Y. Song, J. B. Park, Y. Park, and S. H. Choi, Appl. Phys. Lett. **89**, 083109 (2006).

⁶F. M. Yang, T. C. Chang, P. T. Liu, P. H. Yeh, Y. C. Yu, J. Y. Lin, S. M. Sze, and J. C. Lou, Appl. Phys. Lett. **90**, 132102 (2007).

⁷S. P. Murarka, *Silicide for VLSI Application* (Academic, Orlando, 1983).

⁸Simon M. Sze and Kwok K. Ng, *Physics of Semiconductor Devices* (Wiley, New Jersey, 2007).

⁹Masahiro Katoh and Yohei Takeda, Jpn. J. Appl. Phys., Part 1 **43**, 7292 (2004).

¹⁰O. Kubaschewski and B. E. Hopkins, *Oxidation of Metals and Alloys* (Butterworths, London, 1953).

¹¹R. Beyers, J. Appl. Phys. **56**, 147 (1984).

¹²S. Zirinsky, W. Hammer, F. d'Herule, and J. Baglin, Appl. Phys. Lett. **33**, 76 (1978).

¹³D. K. Sadana, A. E. Morgan, M. H. Norcott, and S. Naik, J. Appl. Phys. **62**, 2830 (1987).